SOME RADAR TOPICS: WAVEFORM DESIGN, RANGE CFAR AND TARGET RECOGNITION

H. Rohling
Technical University Hamburg-Harburg
Hamburg, Germany
rohling@tu-harburg.de

Abstract   The first RADAR patent was applied for by Christian Huelsmeyer on April 30, 1904 at the patent office in Berlin, Germany. He was motivated by a ship accident on the river Weser and called his experimental system "Telemobiloscope". In this chapter some important and modern topics in radar system design and radar signal processing will be discussed. Waveform design is one innovative topic where new results are available for special applications like automotive radar. Detection theory is a fundamental radar topic which will be discussed in this chapter for new range CFAR schemes which are essential for all radar systems. Target recognition has for many years been the dream of all radar engineers. New results for target classification will be discussed for some automotive radar sensors.

Keywords:
automotive radar; continuous wave radar; CFAR processing; rank-order; filters; FSK modulation; matched filters; unmatched filters.

1.   Introduction

The objective of this chapter is to discuss some important contributions to radar system design and digital radar signal processing. The focus is on waveform design in general and on automotive applications in particular. Target detection is an important issue for all radar systems. Therefore some range CFAR (constant false alarm rate) procedures will be discussed which can be applied, especially in multiple target situations, to avoid masking. Additionally some new results are discussed for target recognition systems which have been developed for automotive applications.

2. Combination of LFMCW and FSK modulation principles for automotive radar systems

High performance automotive radar systems are currently under development for various applications. Comfort systems like Adaptive Cruise Control (ACC) are already available on the market as 77 GHz radars. Target range and velocity are measured simultaneously with high resolution and accuracy even in multi-target situations, but the measurement and processing time to detect the relevant object is approximately 100 ms. Future developments will be more concentrated on safety applications like Collision Avoidance (CA) or Autonomous Driving (AD). In this case the requirements for reliability (extreme low false alarm rate) and reaction time (extreme short delay) are much higher compared with ACC systems.

To meet all these system requirements specific waveform design techniques must be considered. For ACC systems both radar types of classical pulse waveform with ultra short pulse length (10 ns) or alternatively continuous wave (CW) transmit signal with a bandwidth of 150 MHz are considered. The main advantage of CW systems in comparison with classical pulse waveforms is the low measurement time and low computational complexity.

This section describes a new waveform design for automotive applications based on CW transmit signals which lead to an extremely short measurement time. The basic idea is a combination of linear frequency modulation (LFM) and FSK CW waveforms in an intertwined technique. Unambiguous range and velocity measurement with high resolution and accuracy can be required in this case even in multi-target situations. After introductions to FSK and LFM waveform design techniques in sections 2 and 1 the combined and intertwined waveform is described in detail in section 1.

PURE FSK MODULATION

Pure FSK modulation (as shown in Figure 1 (a)) uses two discrete frequencies f_A and f_B (so-called two frequency measurement) [1] in the transmit signal. Each frequency is transmitted inside a so-called coherent processing interval (CPI) of length T_{CPI} (e.g. $T_{CPI} = 5$ ms). Using a homodyne receiver the echo signal is down converted by the instantaneous frequency into base band and sampled N times. The frequency step $f_{Step} = f_B - f_A$ is small and will be chosen to depend on the maximum unambiguous target range. The time-discrete receive signal is Fourier transformed in each CPI of length T_{CPI} and targets will be

detected by an amplitude threshold (CFAR). Due to the small frequency step a single target will be detected at the same Doppler frequency position in the adjacent CPI's but with different phase information on the two spectral peaks. The phase difference $\Delta\varphi = \varphi_B - \varphi_A$ in the complex spectra is the basis for the target range (R) estimation. The relation between the target distance and phase difference is given by the equation:

$$R = -\frac{c \cdot \Delta\varphi}{4\pi \cdot f_{Step}}. \tag{1}$$

To achieve an unambiguous maximum range measurement of 150 m a frequency step of $f_{Step} = 1$ MHz is necessary. In this case the target resolution only depends on the CPI length T_{CPI}. The technically simple VCO modulation is an additional advantage of this waveform. But this FSK waveform does not allow any target resolution in the range direction, which is an important disadvantage of this measurement technique. Especially in the automotive traffic environment, more than a single fixed target will occur simultaneously inside an antenna beam. These fixed targets cannot be resolved by a FSK waveform.
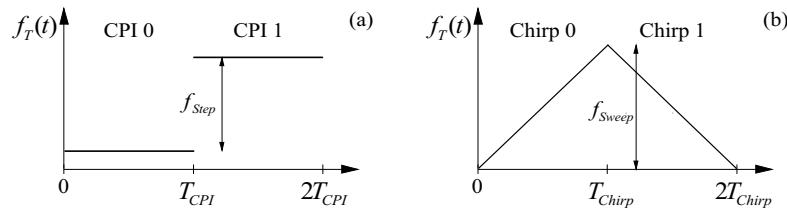

Figure 1. Two CW waveform principles: (a) FSK modulation, (b) LFM

PURE LINEAR FREQUENCY MODULATION

Radars which use a pure LFM technique modulate the transmit frequency with a triangular waveform [6]. The oscillator sweep is given by f_{Sweep}. A typical value for the bandwidth is $f_{Sweep} = 150$ MHz to achieve a range resolution of $\Delta R = \frac{c}{2 \cdot f_{Sweep}} = 1$ m. In general, a single sweep of the LFM waveform gives an ambiguous measurement in range and relative velocity. The down converted receive signal is sampled and Fourier transformed inside a single CPI. If a spectral peak is detected in the Fourier spectrum at index κ (normalized integer frequency) the ambiguities in target range and velocity can be described in an R-v-diagram by the equation:

$$\kappa = \frac{v}{\Delta v} - \frac{R}{\Delta R} \quad \Leftrightarrow \quad \frac{v}{\Delta v} = \frac{R}{\Delta R} + \kappa \tag{2}$$

where Δv gives the velocity resolution resulting from the CPI duration T_{Chirp} ($\Delta v = \frac{\lambda}{2 \cdot T_{Chirp}} = 0.8$ m/s, λ is the wavelength of 4 mm @ 77 GHz and $T_{Chirp} = 2.5$ ms).

Due to resulting range-velocity ambiguities, further measurements with different chirp gradients in the waveform are necessary to achieve an unambiguous range-velocity measurement, even in multi-target situations. The well-known up/down-chirp principle as it is depicted in Figure 1 (b) is described in detail in [5]. LFM waveforms can be used even in multi-target environments, but the extended measurement time is an important drawback of this LFM technique.

COMBINED FSK AND LFM WAVEFORMS

The combination of FSK and LFM waveform design principles offers the possibility of unambiguous target range and velocity measurement simultaneously. The transmit waveform consists in this case of two linear frequency modulated up-chirp signals (the intertwined signal sequences are called A and B). The two chirp signals will be transmitted in an intertwined sequence (ABABAB...), where the stepwise frequency modulated sequence A is used as a reference signal while the second up-chirp signal is shifted in frequency by f_{Shift}. The received signal is down converted into base band and directly sampled at the end of each frequency step. The combined and intertwined waveform concept is depicted in Figure 2.
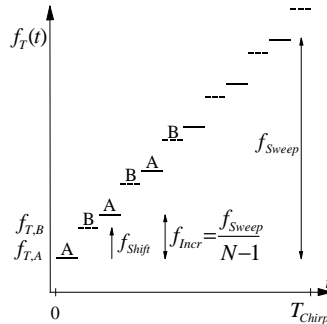

Figure 2. Combined FSK-LFMCW waveform principle.

Each signal sequence A or B will be processed separately by using the Fourier transform and CFAR target detection techniques. A single target with specific range and velocity will be detected in both sequences

at the same integer index $\kappa = \kappa_A = \kappa_B$ in the FFT-output signal of the two processed spectra. In each signal sequence A or B the same target range and velocity ambiguities will occur as described in equation 2. But the measured phases φ_A and φ_B of the two (complex) spectral peaks are different and include the fine target range and velocity information which can be used for ambiguity resolution. Due to the coherent measurement technique in sequences A, B the phase difference $\Delta\varphi = \varphi_B - \varphi_A$ can be evaluated for target range and velocity estimation. The measured phase difference $\Delta\varphi$ can be described analytically by the following equation:
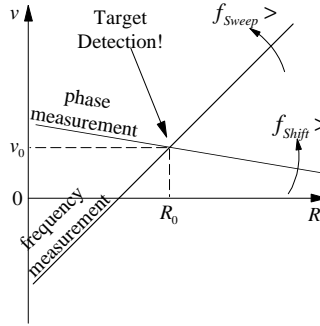

Figure 3. Graphical resolution principle of ambiguous frequency and phase measurements.

$$\Delta\varphi = \frac{\pi}{N-1} \cdot \frac{v}{\Delta v} - 4\pi \cdot R \cdot \frac{f_{Shift}}{c} \tag{3}$$

where N is the number of frequency steps (or receive signal samples) in each transmit signal sequence A, B. In this first step $\Delta\varphi$ is ambiguous but it is possible to resolve these ambiguities by combining the two measurement results of equations 2 and 3. The intersection point of the two measurement results is shown in Figure 3 in a graphical way. The analysis leads to an unambiguous target range R_0 and relative velocity v_0 :

$$R_0 = \frac{c \cdot \Delta R}{\pi} \cdot \frac{(N-1) \cdot \Delta\varphi - \pi \cdot \kappa}{c - 4 \cdot (N-1) \cdot f_{Shift} \cdot \Delta R} \tag{4}$$

$$v_0 = \frac{(N-1) \cdot \Delta v}{\pi} \cdot \frac{c \cdot \Delta\varphi - 4\pi \cdot f_{Shift} \cdot \Delta R \cdot \kappa}{c - 4 \cdot (N-1) \cdot f_{Shift} \cdot \Delta R} \tag{5}$$

This new intertwined waveform shows that unambiguous target range and velocity measurements are possible even in a multi-target environment. An important advantage is the short measurement and processing time.

SYSTEM EXAMPLE

In this section a waveform design based on the new intertwined signal is developed as an example for automotive applications. The signal bandwidth is $f_{Sweep} =$ 150 MHz to fulfill the range resolution requirement of 1 m. The stepwise frequency modulation is split into $N = 256$ separate bursts of $f_{Incr} = \frac{150\text{MHz}}{255} = 588$ kHz each. The measurement time inside a single burst A or B is assumed to be 5 μs resulting in a chirp duration of the intertwined signal of $T_{Chirp} = 2.56$ ms. This results in a velocity resolution of $\Delta v = \frac{\lambda}{2 \cdot T_{Chirp}} = 2.7$ km/h.

The important waveform parameter f_{Shift} is optimized on the basis of high range and velocity accuracy. The highest accuracy occurs if the intersection point in the R-v-diagram results from two orthogonal lines.

For this reason the frequency shift between the signal sequences A and B is $f_{Shift} = -\frac{1}{2} \cdot f_{Incr} = -294$ kHz.

In this specific case equations 4 and 5 turn into

$$\frac{R_0}{\Delta R} = \frac{N-1}{2\pi} \cdot \Delta\varphi - \frac{\kappa}{2} \tag{6}$$

$$\frac{v_0}{\Delta v} = \frac{N-1}{2\pi} \cdot \Delta\varphi + \frac{\kappa}{2} \tag{7}$$

The proposed intertwined and stepwise CW waveforms show high performance in simultaneous range and velocity measurement accuracy. The main advantage is the short measurement time in comparison to classical LFM waveforms while the resolution and accuracy are unchanged. The properties of the new intertwined CW waveform technique are quite promising. This concept is a good basis for high performance automotive radar systems with different safety applications (e.g. pre crash) which require ultra short measurement and processing times.

3.   Automotive Radar Network Based On 77GHz FMCW Sensors

Automotive radar systems need to have the capability to measure range, velocity and azimuth angle simultaneously for all point and extended targets inside the observation area. Short measurement time even in dense target situations, and high range accuracy and resolution, are required in all automotive applications. We will distinguish in this section between single radar sensors and radar network systems. So-called far distance single radar sensors use an observation area of $\pm 10°$ in azimuth angle and a maximum range of up to 200m.

If, in contrast, a large azimuth angle coverage and a short maximum range are required, radar network systems with e.g. four individual sensors mounted behind the front bumper are used instead of a single radar sensor. Typical automotive applications for radar networks with a large azimuth angle coverage but limited range are, for example, Collision Avoidance and Pre Crash Warning. Figure 4 illustrates the observation area considered in this section. The relevant system parameters for a short-range radar network are given in Table 1.

The developed near distance single radar sensor provides target range and radial velocity simultaneously with high accuracy and for all objects inside the observation area. It is characteristic of radar networks signal processing that the angular position of each target is calculated by means of multilateration techniques based on the sensor specific measured target ranges inside the network [7, 8]. This is to derive the desired target position by calculating the intersection point of all range measurements from different radar sensor positions.
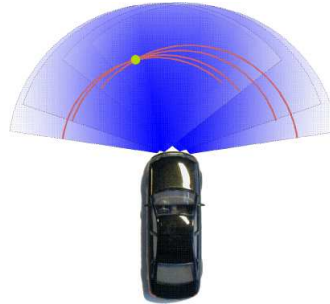

Figure 4.   Observation area of the radar network system.

Table 1.   Requirements for a single sensor in a radar network system

Parameter	Value
Observation area	120° in azimuth
Maximum range	40m
Range resolution	0.4m
Range accuracy (required by multilateration)	0.02m
Velocity resolution	1m/s
Velocity accuracy	0.3m/s
Target acquisition time	20-100ms

RADAR NETWORK

Architecture. In this section we present a short-range radar network that consists of four distributed 77GHz radar sensors [9]. All sensors are mounted behind the front bumper of the vehicle in an invisible form. In contrast to already known radar networks in the 24GHz frequency domain, the presented sensors are working at a 77GHz carrier frequency. Due to European regulations, this frequency band provides a wider bandwidth for automotive radar applications. To achieve the desired high range accuracy of 2cm, which is required by the multilateration process, a frequency sweep of 1GHz has to be utilized within the Linear Frequency Modulated Continuous Waveform (LFMCW). Figure 5 shows an image of the 77GHz prototype sensor [10]. Time synchronization between the individual sensors is needed to avoid any interference situations between the radar sensors. With additional carrier synchronization between the sensors the radar network could even provide the capability of bistatic measurements. The measurement results described in this section are based on monostatic sensor measurements.
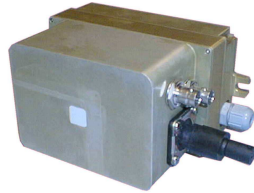

Figure 5. Close-up of a single 77GHz radar sensor.

Experimental system. To validate the analytical results some experimental cars, shown in Figure 6, have been equipped with a radar network. These test cars are used for data acquisition and recording to optimize the signal processing algorithms. In section 9 experimental results are presented to illustrate the theoretical results of developed and applied algorithms.

SINGLE SENSOR SIGNAL PROCESSING

For data acquisition a classical linear FMCW waveform is used which consists of four individual chirp signals (see Figure 7) and covers a bandwidth of 1GHz, which corresponds to a range resolution of 0.4m under realistic signal processing conditions. This waveform combines high ac-

Figure 6. Two experimental cars equipped with 77GHz radar sensors.

curacy measurements in range and velocity and reliable target detection in multi-target situations. Furthermore, FMCW signal processing techniques compared with pulse radar waveforms lead to reduced computational complexity and hardware requirements [11].

Four individual chirps provide sufficient redundancy in multi-target or extended target situations [4] to suppress ghost targets in the range-velocity processing. For each individual chirp signal the beat frequencies $df_1, \dots df_4$, shown in Figure 7, will be estimated by applying an FFT.
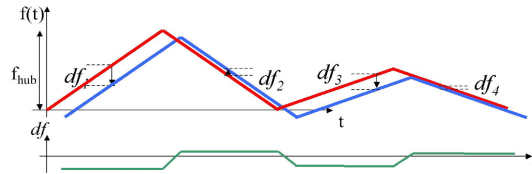

Figure 7. FMCW radar waveform (red) and the corresponding receive signal (blue) for a single target situation.

Table 2 gives a summary of the considered waveform parameters. It is a real technical challenge to handle, in multiple and extended target situations, the large number of detections in the data association, tracking as well as range, velocity and angle parameter estimation procedure. Therefore, a specific signal processing technique has been developed and is implemented in the experimental system.

The classical FMCW radar signal processing scheme is structured into the following different independent blocks: beat frequency estimation based on FFT, target detection (CFAR), range and velocity processing, multilateration for azimuth angle measurement and tracking; see Figure 8 and [12]. Even as an enhancement of classical signal processing a classification procedure could be used to derive additional information about the target object class [13].

Table 2.   Waveform Parameters

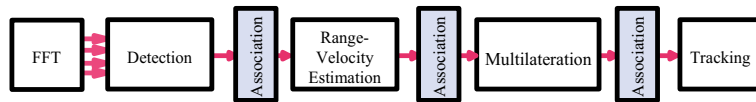| Parameter	Value
Center frequency	77GHz
Number of Chirps	4
Single chip duration	2 ms
First sweep bandwidth	1GHz
Second sweep bandwidth	500MHz

Figure 8.   Classical FMCW radar signal processing

After CFAR detection each signal-processing block contains an independent association procedure to combine measurements from different chirps and different radar sensors, which belong to a single point or even extended target. In the following, all signal processing steps are presented and will be discussed in detail.

The objective of this section is to optimize the classical signal processing structure especially for automotive applications. The main drawback of the classical signal processing structure is that in multiple and extended target situations each of the three independent association procedures (Figure 8) will induce some ghost targets. This network behavior has been observed in many sets of measured data. Based on these observations and results inside a classical radar network an alternative signal processing structure is proposed herein, which is based on a joint optimization of the three independent association schemes.

Target detection.   Due to the large angular coverage considered it is characteristic for automotive applications that each radar sensor has many detections at the CFAR procedure output due to multiple and extended target situations. For reliable target detection in this multi target environment, an ordered-statistic (OS) constant-false-alarm-rate (CFAR) thresholding has been applied which showed the best experimental results [14].

As a result of the FMCW waveform with four individual chirp signals, a proper detection process results in four detected beat frequencies $f_{C,S}$ per point target and sensor. In total a single target, detected by the

radar network, will lead to 16 detected beat frequencies at the FFT output. The vector $\vec{m}^f$ combines these beat frequencies and therefore describes all information which is available in the signal-processing scheme for each individual target.

$$\vec{m}^f = \left[\underbrace{f_{1,1}, f_{2,1}, f_{3,1}, f_{4,1}}_{Sensor1}, \cdots, \underbrace{f_{1,4}, f_{2,4}, f_{3,4}, f_{4,4}}_{Sensor4} \right]^T \tag{8}$$

Range-Velocity Estimation. Each measured beat frequency contains information about the target range and velocity in an ambiguous way. But each individual target with range r_S and velocity v_S leads to a deterministic beat frequency for each chirp signal of the waveform. This beat frequency and the relation to target range and velocity is given by the linear equation:

$$f_{C,S} = a_C \cdot r_S + b_C \cdot v_S. \tag{9}$$

Parameters a_C and b_C depend on chirp characteristics like chirp duration, bandwidth and carrier frequency [6]. Based on the 4 beat frequencies measured by a single sensor the point target range and velocity can be derived simultaneously by an intersection process. In this case and in a single point target situation the four measured frequencies are transformed into target range and velocity, unambiguously. But in multiple or even extended target situations this range velocity calculation could lead to some ghost targets.

Each sensor of the radar network has an individual position behind the front bumper. Therefore, each sensor will calculate individual values for target range and velocity based on the four measured beat frequencies, equation 8, inside the FMCW waveform. The measurement result is described by an eight-element parameter vector.

$$\vec{m}^t = \left[\underbrace{r_1, v_1}_{Sensor1}, \cdots, \underbrace{r_4, v_4}_{Sensor4} \right]^T \tag{10}$$

A set of linear equations can now be derived which describes the relation between 16 measured beat frequencies and sensor specific target range and velocity parameters.

$$\vec{m}^f = C \cdot \vec{m}^t \tag{11}$$

In multi-target situations the association of the detected beat frequencies at the FFT output to different targets is not trivial. Therefore, a

data association process has to be performed using the redundancy given by the four chirp signals inside a single waveform.

RADAR NETWORK SIGNAL PROCESSING

The objective of radar network signal processing is to calculate the azimuth angle (or target position in Cartesian coordinates) of each target in multiple or even extended target situations based on the precise range measurement of each radar sensor. Furthermore the tracking procedure is part of the network processing.

Multilateration Procedure. To derive target position and velocity described by a target state vector in Cartesian coordinates

$$\vec{t} = (t_x, t_y, v_x, v_y)^T \tag{12}$$

a multilateration technique is used. Based on sensor specific range and velocity measurements for each individual point target the state vector can be estimated if the position of each sensor behind the front bumper is taken into account, which is described by the vector:

$$\vec{s} = (s_x, s_y)^T. \tag{13}$$

For each sensor the target range, see (9) , can be calculated by a nonlinear equation if target and sensor Cartesian positions are known.

$$r_S = \sqrt{(t_x - s_x)^2 + (t_y - s_y)^2}. \tag{14}$$

The target radial velocity in (9) can be processed as follows:

$$v_S = \frac{t_x - s_x}{r_S} \cdot v_x + \frac{t_y - s_y}{r_S} \cdot v_y. \tag{15}$$

Combining both equations, the relation between target state vector $\vec{t}$ and the measurement parameter vector $\vec{m}^t$, equation 10, can be formulated by the nonlinear equation

$$\vec{m}^t = h(\vec{t}). \tag{16}$$

The Jacobian matrix

$$H_{\vec{t_0}} = \left. \frac{\partial h(\vec{t})}{\partial \vec{t}} \right|_{\vec{t_0}} \tag{17}$$

is used in an iterative Gauss-Newton algorithm to estimate the target position and velocity in Cartesian coordinates based on the given measurements and a given initial position estimate [15].

At the beginning of the multilateration procedure an association process is integrated to select the sensor specific range and velocity measurements belonging to a single target. In multiple and extended target situations there is high risk of ghost targets due to errors in the association procedure. Furthermore, in situations with low target detection probability the multilateration procedure does not have sufficient information for calculating the target state vector. While the data association for range-velocity processing was provided by four individual chirp signals within the waveform, the data association for multilateration processing is provided by measurements of four individual radar sensors at different positions.

Target Tracking.   Normally radar tracking is based purely on plot-to-track association. In this section we develop a radar network and FMCW waveform specific frequency-to-track association as an extension of the classical tracking procedure. For pulse radar networks a similar idea of range-to-track association schemes have been published in [12]. In this case the multilateration technique is not processed independently and explicitly but is integrated into the tracking procedure which is based on Kalman filtering.

For automotive applications with relative low velocities and a high update rate $1/T$, a pure linear motion model with constant velocity can be considered. The respective state transition matrix A for a constant-velocity trajectory can be used to calculate the predicted target state vector for the next time step by the following equation:

$$\vec{t}_{k+1} = A \cdot \vec{t}_k + \vec{w}_k = \begin{bmatrix} 1 & & T & \\ & 1 & & T \\ & & 1 & \\ & & & 1 \end{bmatrix} \cdot \begin{bmatrix} t_x \\ t_y \\ v_x \\ v_y \end{bmatrix} + \begin{bmatrix} 0 \\ 0 \\ w_x \\ w_y \end{bmatrix}. \quad (18)$$

Here $\vec{t}_k$ is the target state vector at time index k and $\vec{w}_k$ contains two random variables which describe the unknown process error, which is assumed to be a Gaussian random variable with expectation zero and covariance matrix Q. In addition to the target dynamic model, a measurement equation is needed to implement the Kalman filter. This measurement equation maps the state vector $\vec{t}_k$ to the measurement domain. In the next section different measurement equations are considered to handle various types of association strategies.

JOINTLY OPTIMIZED RADAR NETWORK SIGNAL PROCESSING

In general, the tracking procedure starts with an association process to combine the established track parameter with the radar sensor or radar network measurements. Errors in the association process will always lead to ghost targets. But the general requirement for automotive applications is to keep the false alarm probability as low as possible, which underlines the importance of the association process for radar networks.

There are several possibilities in radar networks to design this association process in the tracking procedure:

- The target state vector $\vec{t}_k$ measured by the multilateration procedure can be considered directly as a target plot input of the association process. In this case, the input of the Kalman filter describes the same parameters that the internal state vector does. It is characteristic for the plot-to-track association procedure that the measurement equation contains directly the target state vector $\vec{t}_k$ which is influenced by noise $\vec{n}_k^s$ only:

$$\vec{y}_k^s = [t_x, t_y, v_x, v_y]_k^T + \vec{n}_k^s = \vec{t}_k + \vec{n}_k^s. \tag{19}$$

- Alternatively the radar sensor specific measured ranges and velocities $\vec{m}_k^t$ can be used for a track update. In this case the tracking procedure can even be applied in the low target detection situation where the multilateration process cannot be applied. In the range-velocity-to-track association scheme the corresponding measurement equation is based on range and velocity calculations and has a nonlinear analytical structure,

$$
\begin{aligned}
\vec{y}_k^t &= [r_1, v_1, \cdots, r_4, v_4]_k^T + \vec{n}_k^t \\
&= \vec{m}_k^t + \vec{n}_k^t \\
&= h(\vec{t}_k) + \vec{n}_k^t.
\end{aligned}
\tag{20}
$$

It has to be noted that the measurement values for range and velocity are not uncorrelated according to the LFMCW measurement described in section 8. As a consequence, the observed measurement errors $\vec{n}_k^t$ can also be considered as correlated random variables for a single sensor's data. For 24GHz pulse radar networks, developed also for automotive applications, a similar idea has been described by a range-to-track association scheme [12], because no velocity measurements are provided in such a radar network.

- Finally for an FMCW radar waveform all the measured single beat frequencies $\vec{m}^f$ can be used directly for the association process and track update. This technique will be called frequency-to-track association. In this case each radar detection and beat frequency measurement can be directly integrated into the tracking process. An explicit and independent calculation of the range-velocity parameter and multilateration processing is not necessary in this case. This joint association process reduces the ghost target probability dramatically and improves the radar network performance.

$$
\begin{aligned}
\vec{y}_k^f &= [f_{1,1}, f_{2,1}, \cdots, f_{4,1}, \cdots, f_{4,4}]_k^T + \vec{n}_k^f \\
&= \vec{m}_k^f + \vec{n}_k^f \\
&= C \cdot \vec{m}_k^t + \vec{n}_k^f \\
&= C \cdot h(\vec{t}_k) + \vec{n}_k^f
\end{aligned}
\tag{21}
$$

The vector $\vec{n}_k^f$ describes the unknown additive measurement noise, which is assumed in accordance with Kalman filter theory to be a Gaussian random variable with zero mean and covariance matrix R. Instead of the additive noise term $\vec{n}_k^t$ in equation (20), the errors of the different measurement values are assumed to be statistically independent and identically Gaussian distributed, so

$$
R = E\{\vec{n}_k^f \cdot \vec{n}_k^{fT}\} = \sigma_f^2 \cdot I.
\tag{22}
$$

The term $E\{\cdot\}$ denotes the expected value and I is the identity matrix. This covariance matrix can be derived from the radar sensor characteristics.

The respective Kalman filter equations for the position correction and prediction steps can now be formulated based on equations (18) and (19), (20) or (21) accordingly for the different mentioned association schemes. Since the measurement equation is nonlinear in case of range-velocity-to-track or frequency-to-track association, the Extended Kalman filter is used for this particular application [16].

In Figure 9 a block diagram of the frequency-to-track processing is given. The association procedures are no longer processed step–wise at three different places in the block diagram compared to the general classical radar network scheme described in Figure 8.

Even a small subset of the maximum possible sixteen beat frequencies is sufficient for track update processing based on the frequency-to-track association scheme. Almost all association errors could be avoided in multiple and extended target situations applying this procedure. This
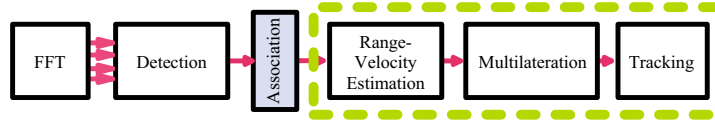
Figure 9.   Block diagram of frequency-to-track association

proposed joint optimization procedure shows increased performance and is additionally quite robust in all situations when some radar sensors in the radar network have low detection probability. The ghost target probability is dramatically reduced.

EXPERIMENTAL RESULTS

As already mentioned, the TUHH experimental car has been equipped with the described 77GHz radar network to validate and prove the efficiency of the derived algorithms. This radar network was used to record measurement data of typical scenarios in real street applications. Based on these recorded data, a comparison of the different signal processing strategies (classical or jointly) for radar network signal processing has been performed.

Typical targets for automotive radar networks are moving cars inside the observation area. Compared with the single radar sensor range resolution of 0.4m a common car cannot be considered any longer as a point but as an extended target. Therefore, each sensor will measure several echo signals in different but closely related range gates for this single car.

Measurements of such extended targets contain and describe all signal processing and association effects discussed in the previous sections.

In the classical signal processing case the target azimuth angle is calculated in the radar network based on multilateration techniques. In this case an extremely high range accuracy of 2cm is required due to the small baseline of radar sensor position inside the network and the required position accuracy. Furthermore, all sensors are observing the car from slightly different aspect angles and can therefore detect different reflection centers. It is obvious that the data association technique becomes very crucial in such situations and the risk of producing ghost targets caused by multiple detections and misassigned measurements in the three independent association schemes is rather high.

On the other hand, the high update rate compared to realistic velocities and accelerations of cars results in a high quality target prediction in the tracking procedure. Therefore, nearest neighbour and gating tech-
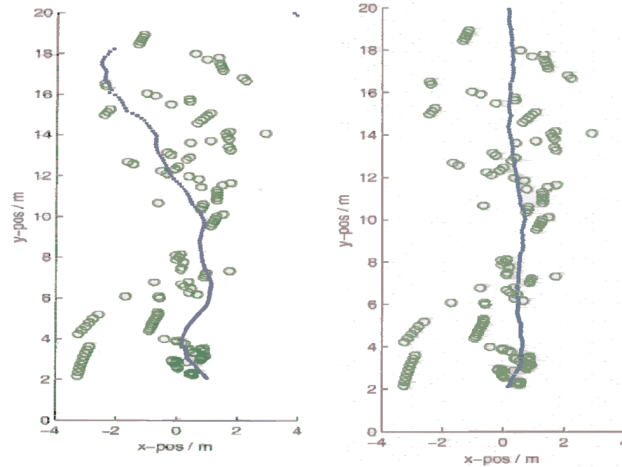
Figure 10. Range-velocity-to-track association with a range gate size of 0.5m and a velocity gate size of 1m/s (left) and frequency-to-track association with a gate size of 1FFT bin (right)

niques with rather small gate sizes can be used for signal processing and association procedures.

As an example, the measurement results of a car driving straight towards the radar-sensor network with a velocity of approximately 5m/s have been analyzed. Figure 10 shows the results of the different signal processing stages. The car can be considered from the single radar sensor point of view as an extended target, which leads to many echo signals with different ranges. Therefore the three association steps in the classical signal processing procedure must be considered quite carefully.

It can be seen that the target positions derived by a pure multilateration procedure (green circles) in the classical signal processing scheme have poor quality and accuracy due to many association errors in the range-velocity measurement inside each sensor and inside the multilateration step. Considering these green dots it is hopeless to establish a plot-to-track association in the tracking procedure.

The situation can be improved by a range-to-track association technique. The blue line in the left part of Figure 10 shows the result of a range-velocity-to track association procedure as described in section 8. In this case the target can be tracked over the complete measurement time but with limited accuracy, especially in the azimuth angle. The target position accuracy is increased for short-range positions.

The right part of Figure 10 shows the result of the joint optimization procedure based on a direct frequency-to-track association as de-

scribed in section 8. The green circles again show the results of a pure multilateration process as in the left part for the extended target measurement situation. The most obvious difference is improved accuracy in angular estimation of the target position. From Figure 10, the improved performance of the proposed joint optimization process and the frequency-to-track association can be seen.

4.   Range CFAR Techniques

The general task of primary radars used in air or vessel traffic control is to detect all targets inside the observation area and to estimate their range, azimuth and radial velocity parameters respectively. The target detection scheme would be an easy task if the echo signal was observed before an empty or statistically completely known noise or clutter signal background. In this case all received echo signal amplitudes would be compared with a fixed threshold, which is based on the noise and clutter statistic only, and targets are detected in all cases when this threshold is exceeded by the echo signal inside the test cell.

But in real radar applications many different noise and clutter background signal situations can occur. The target echo signal practically always appears before a background signal, which is filled with point, area or even extended clutter and additional superimposed noise. Furthermore the location of this background clutter varies in time, position and intensity. Clutter is, in real applications, a complicated time and space variant stochastic process.

All these conditions call for an adaptive procedure in detection and signal processing, operating not with a fixed but with a variable threshold in the detection procedure, to be determined in accordance with the locally observed clutter situation with different range extension, intensity and fluctuation. In a first step of the detection procedure the unknown parameter of a certain statistical background signal is always estimated by analysing the signal inside a fixed window size, which is oriented in the range direction surrounding the radar test cell. The general detection procedure is shown in a block diagram in Figure 11 where the sliding range window is split into two parts, the leading and lagging part surrounding the test cell. Additionally some guard cells are introduced to reduce self-interferences in a real target echo situation.

All data inside the window will be used to estimate the unknown statistical parameters of the background clutter and to calculate the adaptive threshold for target detection. All the background signals, undesired as they are from the standpoint of detection and tracking, are denoted just as "clutter". The detection procedure has to distinguish
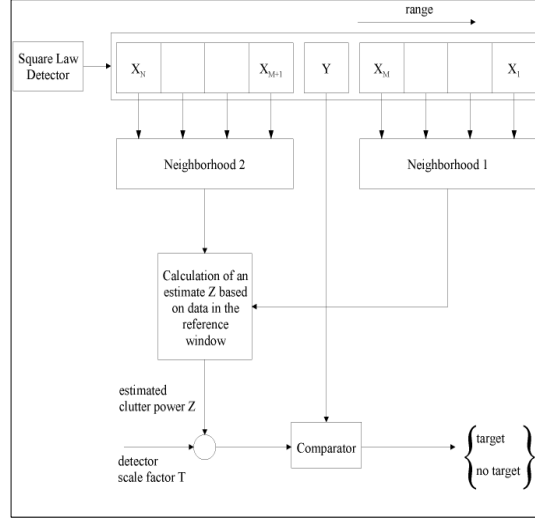
Figure 11. General architecture of range CFAR procedures

between useful target echoes and all possible clutter situations. Clutter is not just a uniformly distributed sequence of random variables but can be caused in practical applications by a number of different physical sources.

Therefore, the length of the sliding window will be chosen as a compromise based on rough knowledge about the typical clutter extension. To get good estimation performance (low variance) in a homogeneous clutter environment the window size N should be as large as possible. But the window length N must be adapted to the typical range extension of homogeneous clutter areas to fulfill the statistical requirement of identically distributed clutter random variables. In typical air traffic control radars the number of range cells is e.g. between N=16 and 32.

Radar target detection in noise

In a first simple model for target detection it is assumed that the background clutter can be described by a statistical model in which the different range cells inside the sliding window contain statistically independent identically exponentially distributed (iid) random variables $\{X_1,\dots,X_N\}$. The probability density function (pdf) of exponentially distributed clutter variables is fully described by the equation:

$$p_0(x) = \quad 1/\mu \ e^{-x/\mu}, \quad x \geq 0. \tag{23}$$

In this ideal case it is assumed that μ is a known parameter which describes the expected value of the exponentially distributed random variables. The variance of the random variable X in this case is $\sigma^2 = \mu^2$. The false alarm probability (P_{fa}) depends on the noise and clutter statistic only and a certain threshold S will be calculated analytically as follows:

$$P_{fa} = \int_{S}^{\infty} p(x)dx \qquad (24)$$

$$S = T \cdot \mu. \qquad (25)$$

The factor T of the threshold S can be described for a given false alarm probability (P_{fa}) in this case analytically by the equation:

$$T = \ln \frac{1}{P_{fa}}. \qquad (26)$$

The non-fluctuating target amplitude statistic can be described by the Rician pdf:

$$p_1(x) = \begin{cases} \frac{x}{\sigma_0^2} e^{-\frac{x^2+c^2}{2\sigma_0^2}} I_0\left(\frac{xc}{\sigma_0^2}\right), & x \geq 0; \\ 0, & \text{otherwise.} \end{cases} \qquad (27)$$

Therefore the detection probability (P_d) for a non-fluctuating target in homogeneous noise is:

$$P_d = \int_{T\mu}^{\infty} p_1(x)dx. \qquad (28)$$

The general objective of all radar detection procedures is to get a constant false alarm rate (CFAR) due to the fact that the test cell almost always contains clutter and noise and only in a very few cases contains radar target echo signals. The statistical model and general detection procedure, in which the detector is fixed only with regard to the noise and clutter statistic and independently to the target statistic, has been developed by Neyman and Pearson.

But in real radar applications the average noise and clutter power level (μ) is unknown and must be estimated in the detection procedure first. This is done by several published CFAR procedures, which will be discussed in this section, where each specific CFAR technique is motivated by assumptions about a specific background signal or target signal model.

Range CFAR procedures with sliding window techniques

Each developed and published CFAR technique refers implicitly to a certain background clutter or even target model. Therefore, in the following these assumptions will be described explicitly and the different CFAR procedures considered will be compared in some clutter situations. The amplitude in each individual range cell is tested. Therefore a window of fixed size is applied to each range cell inside the full range coverage using a sliding technique. The amplitudes in the leading and lagging reference cells are used in a signal processing procedure to estimate the unknown statistical parameters of the clutter background signal. Based on these estimated parameters the detection threshold will be calculated. The different range CFAR techniques differ in the way to estimate the statistical parameters. In the following the background signal model and the resulting motivation for each CFAR technique will be described. Furthermore each range CFAR technique will be applied in four different but (for radar applications) characteristic signal situations which consist of: pure noise; local clutter; single target in noise; and two targets respectively. From these examples the characteristic behavior of each CFAR procedure can be seen clearly.

Cell averaging CA CFAR. In this first signal model it is assumed that the clutter and noise background at the output of a square law detector can be described by statistically independent and identically distributed (iid) exponential random variables with a single exception: the average clutter plus noise power level is unknown. The optimised signal processing technique in this situation, from a statistical point of view, is to calculate an estimation of the clutter power level just by applying the arithmetic mean to the received amplitudes inside the considered window.

$$Z = \left[\frac{1}{N} \sum_{i=1}^{N} X_i \right].$$
(29)

The arithmetic mean Z has excellent estimation performance. The estimation Z is unbiased, which means

$$E \left[\frac{1}{N} \sum_{i=1}^{N} X_i \right] = \frac{1}{N} \sum_{i=1}^{N} E[X_i] = \mu$$

and shows additionally a minimum estimation variance.

$$Var \left[\frac{1}{N} \sum_{i=1}^{N} X_i \right] = \frac{1}{N^2} \sum_{i=1}^{N} Var[X_i] = \frac{1}{N} \mu^2.$$
(30)

The false alarm rate is given by [4] as:

$$P_{fa} = P(Y \geq T_{CA} \cdot Z) = (1 + T_{CA})^{-N}. \tag{31}$$

If this estimation procedure is applied to the random variables inside the range window this CFAR procedure is called "cell averaging," CA-CFAR. The statistical performance is excellent if the assumptions of homogeneous clutter inside the reference window are fulfilled in the statistical model and in the real world application. It is not clear to the author who first analyzed and published this CA-CFAR idea, but Nitzberg [17] published a paper in 1978 analyzing CA-CFAR for fluctuating targets. To demonstrate the general CFAR characteristic some typical signal situations are generated which are considered to be characteristic for radar applications. These are: a pure noise background signal inside the full range coverage; a local clutter area over 10 adjacent range gates superimposed with noise; a single target and a double target situation (20 dB SNR each) superimposed with noise. The clutter power was chosen 13 dB above noise power. Figure 12 shows the resulting threshold S in these noise, clutter and target situations when the CA-CFAR procedure is applied.
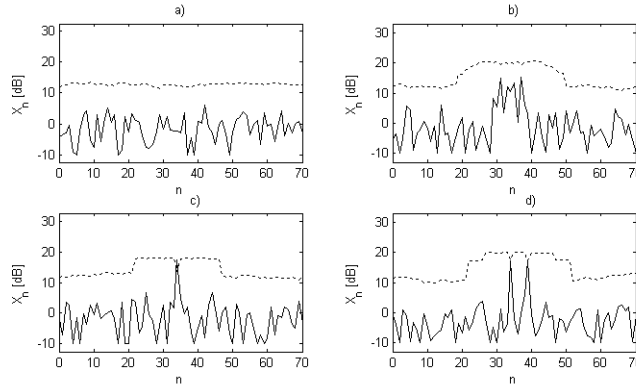

Figure 12. CA-CFAR (N=24), $P_{fa} = 10^{-6}$

Figure 12 shows the appropriately calculated detection threshold in the pure noise situation (12 a). This homogeneous noise model with unknown noise power was the motivation to develop CA-CFAR. The detection procedure adapts quite well in the local clutter with some losses (increased P_{fa}) at the clutter edges (12 b). The characteristic behavior in target situations is not acceptable (12 c). In the two target

situation both targets are not even detected by CA-CFAR due to the resulting masking situation (12 d).

Cell averaging with greatest of CAGO-CFAR. The clutter and noise signals are varying in time and position and the average clutter power level can fluctuate in different range areas and range cells. If a CA-CFAR is applied in the radar detector it may happen that the sliding window is located in the transition between a pure noise and strong clutter area with different average power level, as shown in Figure 12c for example. From a statistical point of view this means that the random variables inside the sliding window are no longer identically distributed but have different expected values μ in their individual statistics. CA-CFAR leads in such cases to an increase in false alarm rate (P_{fa}), which is unacceptable for practical applications and requirements.

Therefore the clutter model is extended and non-homogeneous clutter situations are integrated, such as in typical transition areas between noise and beginning clutter areas. Referring to such realistic clutter situations a new CFAR procedure has been designed by Vilhelm G. Hansen in his well-known paper [18]. In order to demonstrate the advantage of this CFAR technique it is important to recall the CA-CFAR procedure. In this case the arithmetic mean is calculated in the leading and lagging part of the range window and both values are summed up; see Figure 11.
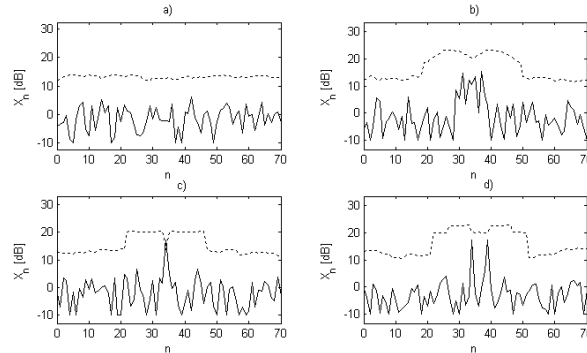

Figure 13. CAGO-CFAR (N=24), $P_{fa} = 10^{-6}$

In the extended CFAR case a cell averaging technique is used in each part of the range window but with a "greatest of" selection (CAGO-CFAR).

$$Z = Max\left(\left[\frac{2}{N}\sum_{i=1}^{N/2}X_i\right], \left[\frac{2}{N}\sum_{i=N/2+1}^{N}X_i\right]\right). \qquad (32)$$

If CAGO-CFAR is applied in such typical clutter situations the false alarm rate is reduced at the clutter edges but the detection rate is simultaneously reduced slightly, see Figure 13.

CAGO-CFAR shows a clear advantage in typical transition areas between pure noise and strong clutter or between two different clutter regions. But it simultaneously reduces the sensitivity in target detection in a homogeneous clutter situation. This is a compromise, which always occurs in radar detection due to the variety of different noise and clutter background situations, which can occur in real radar applications. It is a useful extension of CA-CFAR but shows the same characteristics in multiple target situations.

Moshe Weiss [25] developed an extension of CAGO-CFAR to get better performance in multiple target situations and designed cell averaging CFAR with smallest of (CASO-CFAR) procedures and analysed the performance especially in multiple target situations.

These CFAR procedures suffer from the fact that they are specifically tailored to the assumption of uniform and homogeneous clutter inside the reference window. Based on these assumptions, they estimate the unknown clutter power level using the unbiased and most efficient arithmetic mean estimator. Improved CFAR procedures should be robust with respect to different clutter background and target situations. Also in non-homogeneous situations CFAR techniques should remain able to provide reliable clutter power estimations.

OS-CFAR. Applying CAGO-CFAR in the detection procedure brings several advantages in clutter transition areas. But the CA and CAGO-CFAR detection procedures behave very sensitively in multiple target situations and show pure performance. This observation has been described in [14]. It was shown that even in a two-target situation it is possible that both targets are masked by each other. Weak targets in the neighbourhood of strong targets are masked in almost all cases, which reduces the range resolution and is not acceptable in real radar applications. The "ordered statistic" OS-CFAR has in all these multiple target situations a much better performance compared to CA and CAGO-CFAR procedures.

OS-CFAR is not based on the assumption of homogeneous clutter inside the reference window. Therefore the window length can be extended in the OS-CFAR case without any disadvantages. For comparison, OS-CFAR with $N = 24$ will even outperform classical CA-CFAR

with $N = 16$. This is an important advantage of the OS-CFAR procedure.

The general idea of an ordered statistic is technically simple. To estimate the average noise and clutter power a single rank $X_{(k)}$ of the ordered statistic is used instead of the arithmetic mean. In this case a very few large amplitudes in the sliding window have a very small effect on the estimation result. OS-CFAR is robust in multiple target situations. The threshold is hardly influenced by a second or third target inside the window.

All amplitudes inside the sliding window are sorted according to increasing magnitude.

$$X_{(1)} \leq X_{(2)} \leq \cdots \leq X_{(N)}$$
$$Z = X_{(k)}. \tag{33}$$

The pdf of the kth value of the ordered statistic is given by

$$P_{X_{(k)}}(x) = p_k(x) = k \left(\begin{array}{c} N \end{array} \right) (1 - P_X(x))^{N-k} (P_X(x))^{k-1} p_x(x). \tag{34}$$

Thus the pdf of the kth value of the ordered statistic for exponentially distributed random variables is given by

$$P_{X_{(k)}}(x) = p_k(x) = k/\mu \left(\begin{array}{c} N \end{array} \right) \left(e^{-x/\mu} \right)^{N-k+1} (1 - e^{-x/\mu})^{k-1}. \tag{35}$$

The relation between P_{fa} and T_{OS} can be calculated by combining (2) and (13)

$$P_{fa} = k \begin{pmatrix} N \\ k \end{pmatrix} \frac{(k-1)! \ (T_{OS} + N - k)!}{(T_{OS} + N)!}. \tag{36}$$

The importance of this case is that OS-CFAR can be analytically analysed without any approximations. Furthermore the resulting scaling factor T_{OS} is completely independent of μ. Figure 14 shows the typical behaviour of OS-CFAR in clutter edge and multiple target situations. The threshold follows the clutter contour with a certain safety distance. In two target situations the threshold is more or less unchanged compared with a pure noise situation.

Nadav Levanon [21, 22] has applied OS-CFAR to a Weibull distributed background signal and described the results analytically. Blake [26] analysed OS-CFAR in non-uniform clutter. Weber and Haykin [24] have extended OS-CFAR to a two parameter distribution with variable skewness.
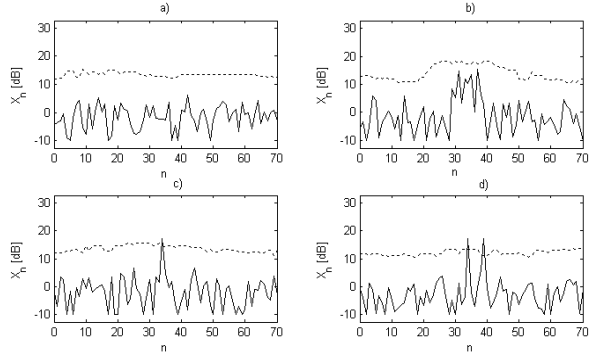
Figure 14. OS-CFAR (N=24), k=3/4*N, $P_{fa} = 10^{-6}$

In [28] the performance of OS-CFAR in a 77GHz radar sensor for car application is examined. In the automotive radar application case multiple target situations occur almost always.

OSGO-CFAR. An extension of OS-CFAR has been developed by He You in his paper [20]. In this case an ordered statistic is applied in the left and right window part separately followed by a greatest of selection. Therefore, the procedure is called OSGO CFAR. The computational complexity is reduced in this case and the detection performance shown in Figure 15 is good.

Gaspare Galati et. al. compared the performance of OS-CFAR and OSGO CFAR in the presence of different backgrounds [23]. He found that the OSGO method suffers only a small additional loss with respect to the OS. In a non-homogeneous background with clutter edges it even shows superiority in the control of the false alarm probability.

Censored CFAR. Richard and Dillard [19] have proposed a CFAR procedure which is based on CA-CFAR but is already close to the general OS-CFAR idea when they are calculating the largest m values inside the sliding window and excluding these values from the arithmetic mean calculation. This step makes modified CA-CFAR less sensitive in multiple target situations. In their paper they analysed a Censored-CFAR detector for m equals 1 and 2.
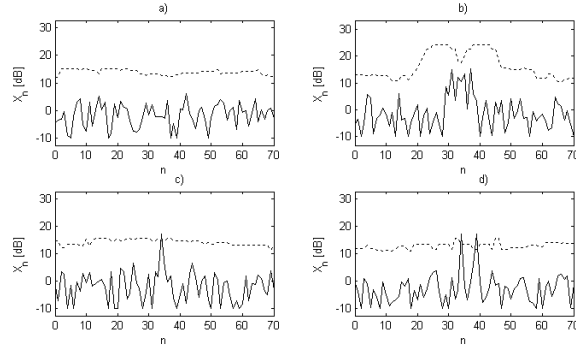
Figure 15.   OSGO-CFAR (N=24), k=3/4*N, $P_{fa} = 10^{-6}$

The resulting false alarm probability for m=1 can also be calculated independently of the actual noise level:

$$P_{fa} = (N-1) \cdot \left\{ \frac{N}{N-1} \sum_{k=1}^{N-1} \binom{N-1}{k} (-1)^{k+1} (1+k+T)^{-1} \right\}^{N-1} . \quad (37)$$

Figure 16 demonstrates the performance of a censored-CFAR detector with m=1. Compared with CA-CFAR the results here are better, because in all scenarios the targets are detected. But compared with OS-CFAR the threshold in the 2 target scenario is still too high in the neighborhood of the targets. Ritcey [29] studied the performance of this method for multiple target situations.
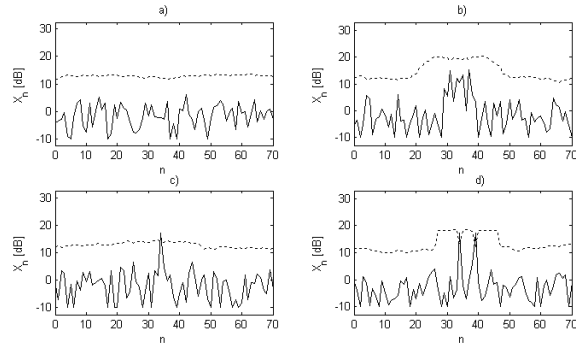

Figure 16.   Censored-CFAR (N=24), k=1, $P_{fa} = 10^{-6}$

WCA-CFAR. If a-priori information about the target position is made available by the tracking system the adaptive threshold can be lowered. A CFAR method called weighted CA-CFAR uses this and was proposed by Barkat, Himonas and Varshney [30].

This method separates the window cells into a leading and a lagging part. Before the mean values of these parts are averaged, they are weighted by the factors α and β. Optimum values for α and β are calculated in accordance with the level of interference of present targets, so that a constant false alarm rate and a high detection probability can be guaranteed.

Other publications. Many additional papers have been published which are based on the four fundamental procedures – CA-, OS-, GO- and SO-CFAR. In these publications either new combinations and modifications of existing procedures or the performance in new environments are analysed.

The main relevant models for radar detection are

- Pure clutter or noise situations with fully homogeneous statistic

- Transition between noise and clutter or between two clutter areas with different average power

- Non-homogeneous clutter

- Correlated clutter

- Different clutter amplitude statistics (Rayleigh, Weibull, . . .)

- Different target amplitude statistics (Rice, Swerling models, . . .)

- Single target situations

- Two or multiple target situations.

A simple quantitative comparison between different CFAR procedures in pure clutter and noise situations, which is the most important situation, can be calculated using the average detection threshold (ADT) [14].

In this case the expectation of all calculated thresholds is calculated and can be used for system comparison.

5.   Conclusion

The objective of this chapter was to discuss some important contributions for radar system design and digital radar signal processing. The

focus was on waveform design in general and on automotive applications in particular. Target detection is an important issue for all radar systems. Therefore some range CFAR procedures have been discussed which can be applied especially in multiple target situations to avoid any masking situations. Additionally some new results have been discussed for target recognition.

References

[1] Artis, Jean-Paul; Henrio, Jean-François: *Automotive Radar Development Methodology*, International Conference on Radar Systems, Brest, France, 1999.

[2] Klotz, Michael; Rohling, Hermann: *A high range resolution radar system network for parking aid applications*, International Conference on Radar Systems, Brest/ France, 1999.

[3] Klotz, Michael; Rohling, Hermann: *24 GHz Radar Sensors for Automotive Applications*, International Conference on Microwaves and Radar, MIKON2000, Wrocław/ Poland, 2000.

[4] Rohling, Hermann; Meinecke, Marc-Michael; Mende, Ralph: *A 77 GHz Automotive Radar System for AICC Applications*, International Conference on Microwaves and Radar, MIKON98, Workshop, Kraków/ Poland, 1998.

[5] Rohling, Hermann; Meinecke, Marc-Michael; Klotz, Michael; Mende, Ralph: *Experiences with an Experimental Car controlled by a 77 GHz Radar Sensor*, International Radar Symposium, IRS98, München, 1998.

[6] Stove, A. G.: *Linear FMCW radar techniques*, IEE Proceedings-F, Vol. 139, No. 5, Oct. 1992.

[7] H. Rohling, A. Höß and U. Lübbert: *Multistatic Radar Principles for Automotive RadarNet Applications*, IRS 2002 International Radar Symposium, Bonn, Germany, 2002, pp. 181–185.

[8] M. Schiementz, F. Fölster and H. Rohling: *Angle Estimation Techniques for different 24GHz Radar Networks*, IRS 2003 International Radar Symposium, Dresden, Germany, 2003, pp. 405–410.

[9] A. Hoess et al.: *The RadarNet Project*, 7th ITS World Congress, Torino, November 2000.

[10] Brian Ricket: *A Vision Of Future Applications For An Automotive Radar Network*, WIT 2004, 1st International Workshop on Intelligent Transportation, Hamburg, Germany, 2004, pp. 117-121.

[11] N. Levanon: *Radar Principles*, Wiley & Sons, New York, 1988.

[12] D. Oprisan and H. Rohling: *Tracking Systems for Automotive Radar Networks*, IEE Radar 2002, Edinburgh, UK.

[13] H. Rohling, F. Fölster, F. Kruse and M. Ahrhold: *Target Classification Based on a 24GHz Radar Network*, Radar 2004 Conference, Toulouse, France.

[14] H. Rohling: *Radar CFAR Thresholding in Clutter and Multiple Target Situations*, IEEE Trans. Aerosp. Electron. Syst. 19 No. 4, 1983, pp. 608-621.

[15] M. Klotz: *An Automotive Short Range High Resolution Pulse Radar Network*, PhD thesis, TU Hamburg-Harburg, 2002.

[16] S. Blackman and R. Popoli: *Design and Analysis of Modern Tracking Systems*, Artech House, Boston, 1999.

[17] Nitzberg R.: *Analysis of the Arithmetic Mean CFAR Normalizer for Fluctuating Targets*, IEEE Transactions on AES, 1, pp. 44-47, 1978.

[18] Hansen, V.G., Sawyer, J.H.: *Detectability loss due to greatest of selection in a cell-averaging CFAR*, IEEE Transactions on AES, 16, pp. 115-118, 1980.

[19] Richard, J.T., Dillard, G.M.: *Adaptive Detection Algorithms for Multiple Target Situations*, IEEE Transactions on AES, 4, pp. 338-343, 1977.

[20] He You: *Performance of Some Generalized Modified Order Statistics CFAR Detectors with Automatic Censoring Technique in Multiple Target Situations*, IEE Proceedings F, 131(4), pp. 205-212, 1994.

[21] Levanon, N.: *Detection loss due to interfering targets in ordered statistic CFAR*, IEEE Transactions on AES, (11/1988), pp. 678-681, 1988.

[22] Levanon, N., Shor, M.: *Order statistic CFAR for Weibull background*, IEE Proceedings, F, 137, 3 (6/1990), pp. 157-162, 1990.

[23] Di Vito, A., Galati, G., Mura, R.: *Analysis and comparison of two order statistics CFAR systems*, IEE Proceedings, F, 141, 2 (4/1994), pp. 109-115, 1994.

[24] Weber, P., Haykin, S.: *Ordered statistic CFAR processing for two-parameter distribution with variable skewness*, IEEE Transactions on AES, AES-21, 6 (11/1985), pp. 819–821, 1985.

[25] Weiss, M.: *Analysis of some modified cell-averaging CFAR processors in multiple-target situations*, IEEE Transactions on AES, 18, pp. 102-114.

[26] Blake, S.: *OS-CFAR theory for multiple targets and nonuniform clutter*, IEEE Transactions on AES, 24, 6 (11/1988), pp. 785-790, 1988.

[27] Gini, F., Farina, A., Greco, M.: *Selected List of References on Radar Signal Processing*, IEEE Transactions on AES, 37, 1 (1/2001), pp. 329-359, 2001.

[28] Rohling, H., Mende, R.: *OS CFAR performance in a 77GHz Radar Sensor for Car Application*, CIE International Conference on Radar, Peking, China, 1996.

[29] Ritcey, J. A.: *Censored mean-level detector analysis*, IEEE Transactions on Aerospace and Electronic Systems, AES-22, 3 (July 1986), pp. 443-454, 1986.

[30] Barkat, M., Himonas, S.D., Varshney, P.K.: *CFAR detection for multiple target situations*, IEE Proceedings, F, 136, 5 (10/1989), pp. 193-209, 1989.